

Quaternary ligand binding to aromatic residues in the active-site gorge of acetylcholinesterase

M. HAREL*, I. SCHALK†, L. EHRET-SABATIER†, F. BOUET‡, M. GOELDNER†, C. HIRTH†§, P. H. AXELSEN*¶, I. SILMAN||, AND J. L. SUSSMAN*

Departments of *Structural Biology and †Neurobiology, Weizmann Institute of Science, Rehovot 76100, Israel; ‡Laboratoire de Chimie Bio-organique, Université Louis Pasteur Strasbourg, BP 24, 67401 Illkirch Cedex, France; §Service de Biochimie, Laboratoire d'Ingénierie des Protéines, Centre d'Etudes Nucléaires Saclay, 91191, Gif-sur-Yvette Cedex, France

Communicated by Jean-Marie Lehn, May 10, 1993

ABSTRACT Binding sites of *Torpedo* acetylcholinesterase (EC 3.1.1.7) for quaternary ligands were investigated by x-ray crystallography and photoaffinity labeling. Crystal structures of complexes with ligands were determined at 2.8-Å resolution. In a complex with edrophonium, the quaternary nitrogen of the ligand interacts with the indole of Trp-84, and its *m*-hydroxyl displays bifurcated hydrogen bonding to two members of the catalytic triad, Ser-200 and His-440. In a complex with tacrine, the acridine is stacked against the indole of Trp-84. The bisquaternary ligand decamethonium is oriented along the narrow gorge leading to the active site; one quaternary group is apposed to the indole of Trp-84 and the other to that of Trp-279, near the top of the gorge. The only major conformational difference between the three complexes is in the orientation of the phenyl ring of Phe-330. In the decamethonium complex it lies parallel to the surface of the gorge; in the other two complexes it is positioned to make contact with the bound ligand. This close interaction was confirmed by photoaffinity labeling by the photosensitive probe ³H-labeled *p*-(*N,N*-dimethylamino)benzenediazonium fluoroborate, which labeled, predominantly, Phe-330 within the active site. Labeling of Trp-279 was also observed. One mole of label is incorporated per mole of AcChoEase inactivated, indicating that labeling of Trp-279 and that of Phe-330 are mutually exclusive. The structural and chemical data, together, show the important role of aromatic groups as binding sites for quaternary ligands, and they provide complementary evidence assigning Trp-84 and Phe-330 to the "anionic" subsite of the active site and Trp-279 to the "peripheral" anionic site.

Acetylcholinesterase (AcChoEase, acetylcholine acetylhydrolase, EC 3.1.1.7) terminates transmission at cholinergic synapses by rapid hydrolysis of acetylcholine (AcCho) (1). Symptomatic treatment of diseases whose etiology involves AcCho depletion can be achieved by controlled inhibition of AcChoEase. Anticholinesterase agents are thus of therapeutic importance (2), and they are under active consideration for managing Alzheimer disease (3). The active site of AcChoEase comprises an esteratic subsite, containing the catalytic machinery, and an "anionic" subsite, which binds the quaternary group of AcCho (4). A second, "peripheral," anionic site exists, so named because it appears to be distant from the active site (5, 6). Bisquaternary AcChoEase inhibitors are believed to derive their enhanced potency, relative to similar monoquaternary ligands (7), from the ability to span the two "anionic" sites, ≈14 Å apart (8, 9). The three-dimensional structure of AcChoEase reveals that, like other serine hydrolases, it contains a catalytic triad (10). This triad is located at the bottom of a deep and narrow cavity, named the "aromatic gorge," since ≈40% of its lining is

composed of the rings of 14 conserved aromatic amino acids. Docking studies suggested that the primary site of interaction of the quaternary group of AcCho is with the aromatic ring of a conserved tryptophan, Trp-84 (10). This agreed with earlier spectroscopic and labeling studies (11, 12), as well as with its affinity labeling (13). We present below x-ray crystallographic** and photoaffinity labeling evidence showing the presence of Trp-84 and Phe-330 in the "anionic" subsite of the active site and suggesting that a distal residue, Trp-279, near the top of the gorge, is also involved in ligand binding and may be part of the "peripheral" anionic site.

MATERIALS AND METHODS

Chemicals. Dithiothreitol, acetylthiocholine iodide, 5,5'-dithiobis(2-nitrobenzoic acid), and tetramethylammonium (TMA) bromide were purchased from Aldrich; edrophonium (EDR) chloride, tacrine (THA), and decamethonium (DECA) bromide were from Sigma; and bovine pancreatic trypsin (sequencing grade) was from Boehringer Mannheim. ³H-labeled *p*-(*N,N*-dimethylamino)benzenediazonium fluoroborate ([³H]DDF; 5 Ci/mmol; 1 Ci = 37 GBq) was prepared as described (15). AcChoEase for the crystallographic studies was the G₂ form, from *Torpedo californica* (16), and for photolabeling it was the G₄ form from *Torpedo marmorata* (15).

Crystallographic Data Collection and Refinement. Crystal-line complexes with EDR, THA, and DECA were obtained by soaking the appropriate ligand, dissolved in crystallization mother liquor, into native crystals of *T. californica* AcChoEase at 19°C. Thus, EDR·AcChoEase was obtained by soaking the native crystals in 10 mM EDR chloride in 65% saturated (NH₄)₂SO₄/0.36 M sodium phosphate, pH 6.3, for 14 days. THA·AcChoEase was similarly obtained by using a 2 mM solution for 2 days, and DECA·AcChoEase, by using 10 mM ligand for 7 days. X-ray data sets were collected as for native crystals (10). Structures were determined by using the difference Fourier technique and were refined as for native AcChoEase (10). All *F*_o > 0σ in the range of 6- to 2.8-Å resolution were used for refinement, while all *F*_o > 0σ in the

Abbreviations: AcCho, acetylcholine; AcChoEase, acetylcholinesterase; TMA, tetramethylammonium; EDR, edrophonium; THA, tacrine; DECA, decamethonium; DDF, *p*-(*N,N*-dimethylamino)benzenediazonium fluoroborate.

¶On leave from: Department of Biochemistry and Molecular Biology, Mayo Clinic, Rochester, MN 55905.

§Deceased, May 28, 1992.

**Atomic coordinates of the three AcChoEase complexes have been deposited in the Protein Data Bank, Chemistry Department, Brookhaven National Laboratory, Upton, NY (14), and will be held for one year (references for the THA, EDR, and DECA complexes are 1ACJ, 1ACK, and 1ACL, respectively). They are available immediately to academic users from J.L.S.; nonacademic users should contact the Yeda Research and Development Co. Ltd. at the Weizmann Institute of Science.

The publication costs of this article were defrayed in part by page charge payment. This article must therefore be hereby marked "advertisement" in accordance with 18 U.S.C. §1734 solely to indicate this fact.

range of 20- to 2.8-Å resolution were used for difference Fourier maps. For each complex, ($F_o - F_c$) maps were computed after initial refinement of the native protein coordinates (in the absence of the ligand) by simulated annealing (17). Stereochemistry of all three complexes was very good, with rms deviations in bond lengths < 0.02 Å, and in bond angles < 4°.

Covalent Labeling with [³H]DDF. Preparative photolabeling of purified *T. marmorata* AcChoEase was performed in 50 mM sodium phosphate buffer, pH 7.2, by energy transfer at 295 nm (100 μV) for 20 min at 10°C. Total volume for each irradiation was 2 ml, and final concentrations were AcChoEase at 300 μg/ml, 40 μM [³H]DDF and, in protection experiments, either 0.1 M TMA or 5 μM EDR. After irradiation, 10 mM dithiothreitol was added to destroy unreacted [³H]DDF. Free radioactive ligand was removed by extensive dialysis against 50 mM phosphate buffer before lyophilization.

Proteolytic Cleavage. Modified AcChoEase was redissolved in 2 M urea/0.1 M Tris·HCl, pH 8.5, at a final concentration of 1.1 mg/ml. Trypsin was added periodically, up to a 1:20 (wt/wt) trypsin-to-AcChoEase ratio, in the course of 24 hr at 37°C.

Peptide Separation. Tryptic digests were loaded onto a reverse-phase HPLC column (Vydac C₁₈, 250 × 4.6 mm). Peptides were eluted by a linear gradient of 0–80% (vol/vol) CH₃CN in 0.1% trifluoroacetic acid, in 100 min, at a flow rate of 1.5 ml/min. Selected labeled peaks were rechromatographed on the same column preequilibrated with solvent A [5% 1-propanol/10% CH₃CN/0.1% heptafluorobutyric acid, vol/vol]. A linear gradient was developed from 0% to 70% solvent B [30% 1-propanol/60% CH₃CN/0.1% heptafluorobutyric acid, vol/vol] in 140 min, at a flow rate of 1 ml/min.

[³H]DDF Incorporation. To study [³H]DDF incorporation as a function of the degree of inactivation of AcChoEase, irradiation was performed for various times. For each time, residual activity was measured (18), and the labeling pattern was analyzed by proteolysis and HPLC.

Protein Sequencing. For loading, peptides were dissolved in 70% (vol/vol) formic acid. Automated Edman degradation was carried out on an Applied Biosystems 477A liquid-phase sequencer, using standard cycle programs. Aliquots of the phenylthiohydantoin derivatives of amino acids released at each cycle were analyzed on-line by using an Applied Biosystems 120A reverse-phase HPLC system. The remaining output from each cycle was used to determine radioactivity.

RESULTS AND DISCUSSION

Crystalline ligand·AcChoEase complexes were obtained by soaking the ligands into native crystals. The ligands were as follows: (i) EDR [ethyl(3-hydroxyphenyl)dimethylammonium], a powerful competitive inhibitor of AcChoEase (19) used clinically to diagnose myasthenia gravis (1). Since EDR is quaternary, it does not penetrate cell membranes or the blood–brain barrier, acting primarily at peripheral sites (2). (ii) THA (1,2,3,4-tetrahydro-9-aminoacridine), also a potent competitive inhibitor of AcChoEase (20). Due to its tertiary character, it penetrates the blood–brain barrier, and it is a promising candidate for treating Alzheimer disease (21). (iii) DECA, a bisquaternary ligand, is both a depolarizing neuromuscular blocker and an anticholinesterase (22).

DECA·AcChoEase Complex. Crystals obtained by soaking DECA into the native crystals displayed an elongated electron density within the gorge consistent with that expected for a DECA molecule (Fig. 1A). We see, however, only small differences between the electron density map for these crystals and that for “native” crystals previously regarded as representing an unliganded form (10). This suggests that DECA, which had been used to elute AcChoEase from the

affinity column used for its purification (16), had remained bound in the active site gorge of “native” AcChoEase, perhaps at lower occupancy, despite prolonged dialysis. In the complex, DECA assumes a curved shape along the gorge, with a mixture of *trans* and *gauche* rotamers along its length. Apart from space adequate to accommodate five or six water molecules, DECA defines and fills the volume of the gorge. Both quaternary groups are in van der Waals contact with tryptophan indole rings. One is apposed to that of Trp-84 at the base of the gorge; the distal quaternary group is apposed similarly to the indole of Trp-279, ≈12 Å distant, at the top of the gorge, and appears to have a slight effect on its conformation.

EDR·AcChoEase Complex. The quaternary group of EDR nestles adjacent to the indole of Trp-84, a position virtually equivalent to that of the proximal quaternary group of DECA (Fig. 1B). Trp-84 is covalently labeled by aziridinium (13), which is similar in structure to EDR, and EDR protects against labeling by aziridinium. Our data thus demonstrate good correspondence between the crystal structure and that in solution. The *m*-hydroxyl group is positioned between N^{ε2} of His-440 and O^γ of Ser-200, making hydrogen bonds of 3.0 and 3.5 Å, respectively, to two of the three members of the catalytic triad (see Fig. 1B). There is also a 3.5-Å hydrogen bond to N of Gly-119, which is part of the oxyanion hole (not shown). This provides a structural basis for the observation that such *m*-substituted anilinium ions are potent competitive inhibitors of AcChoEase (19).

THA·AcChoEase Complex. In the THA·AcChoEase complex, THA is stacked against Trp-84, its ring nitrogen hydrogen-bonding to the main-chain carbonyl oxygen of His-440 (3.1 Å); its amino nitrogen forms a hydrogen bond to a water molecule (Fig. 1C). This agrees with earlier solution studies identifying tryptophan in the active site of AcChoEase (12, 13). Moreover, our finding that the three-ring structure of THA is stacked against the indole of Trp-84 agrees with the observation that *N*-methylacridinium forms a charge-transfer complex with a tryptophan in the active site of AcChoEase (11).

The overall conformations of AcChoEase in the EDR·AcChoEase and THA·AcChoEase complexes are similar to the conformation of the DECA·AcChoEase complex. In all three complexes, the only residue undergoing conspicuous conformational change is Phe-330 (Fig. 2). In DECA·AcChoEase, it lies parallel to the methylene chain of DECA and thus to the gorge axis. In EDR·AcChoEase, Phe-330 is slightly rotated about χ_2 and is in contact with the ethyl substituent of EDR. In THA·AcChoEase, the ring of Phe-330 is rotated about both χ_1 and χ_2 , lying parallel to and in contact with THA. THA is thus sandwiched between the rings of Phe-330 and Trp-84. Since there is at least partial occupancy by DECA in the native crystal (see above), the position of Phe-330 in the absence of ligand remains to be established.

Photoaffinity Labeling. Photolabeling of AcChoEase and the AcCho receptor by DDF has yielded valuable information about the amino acid residues participating in AcCho-binding pockets. DDF, which, in the dark, is a reversible competitive antagonist of both AcChoEase and the nicotinic AcCho receptor, attaches covalently upon photoactivation (12, 23). Due to the high reactivity of the photogenerated aryl cation, it is a very efficient topographical probe of both these AcCho-binding proteins (24–26).

For *T. marmorata* AcChoEase, [³H]DDF incorporation was a linear function of the extent of inactivation (Fig. 3). One molecule of [³H]DDF incorporated per active site (0.93 ± 0.11 , $n = 7$) sufficed to block enzymic activity completely. It had been shown previously that TMA could completely protect *Torpedo* AcChoEase from photoinactivation by DDF, demonstrating that labeling was specific (15).

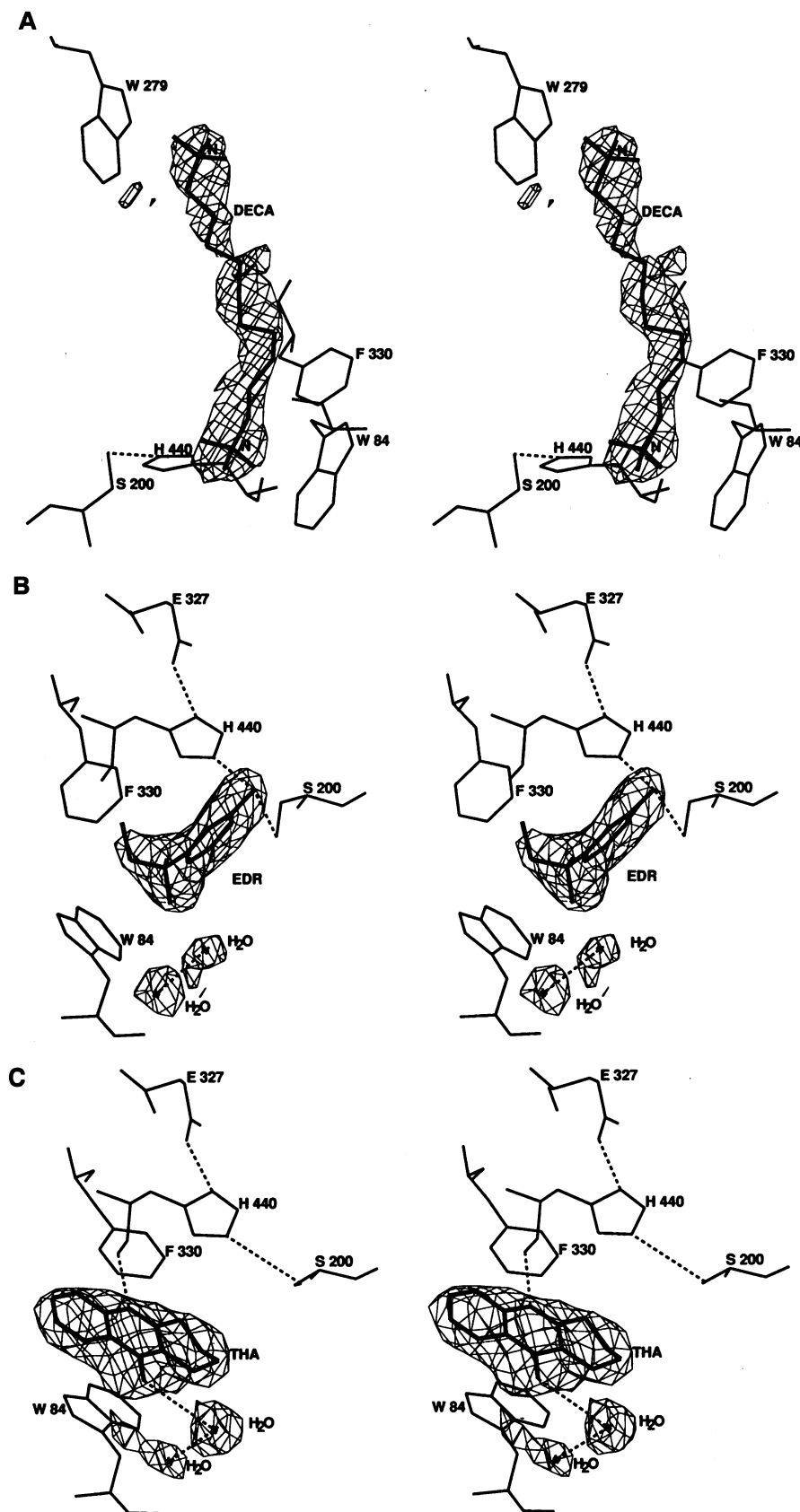


FIG. 1. Initial stereo ($F_o - F_c$) electron density maps, at 2.8-Å resolution, of DECA·AcChoEase (A), EDR·AcChoEase (B), and THA·AcChoEase (C). Maps were contoured at 3.5σ (A) or 3.9σ (B and C) after refinement of the native protein coordinates (in the absence of the ligands; see *Materials and Methods*). The final refined coordinates of the complexes, $R = 19.9\%$ (A), 17.9% (B), and 18.4% (C), are superimposed on the corresponding electron density maps. Broken lines indicate hydrogen bonds.

Identification of Labeled Residues. To identify the site(s) labeled by [³H]DDE, labeled AcChoEase was subjected to

tryptic digestion followed by HPLC. This revealed seven labeled "massifs" (Fig. 4). TMA (0.1 M) abolished incorpo-

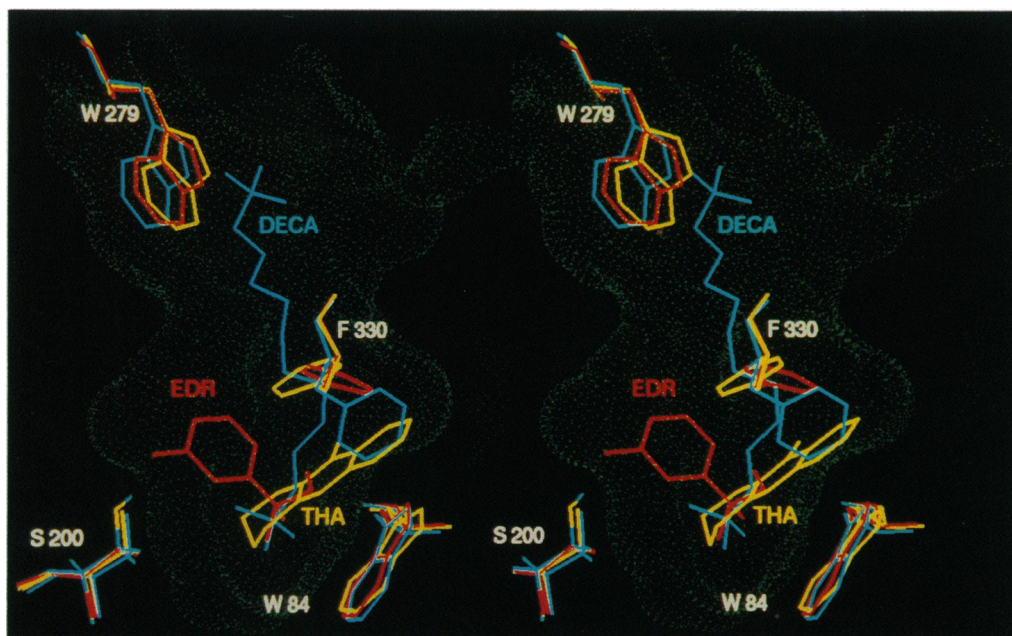


FIG. 2. Stereoview of the overlap of the conserved aromatics in the active site gorge, the catalytic triad residues, and the inhibitor molecules in the refined structures of DECA·AcChoEase (blue), EDR·AcChoEase (red), and THA·AcChoEase (yellow), showing the local conformational changes in Phe-330 and Trp-279. The orientation is similar to that in Fig. 1A, and the van der Waals surface of the gorge is depicted by green dots.

ration of radioactivity into all seven, whereas EDR (5 μM) prevented incorporation into only five. The EDR concentration was chosen to fully occupy the active site ($K_d = 0.25 \mu\text{M}$) (6), but not the "peripheral" site ($K_d = 400 \mu\text{M}$) (27); this suggests that the peptides of massifs 4 and 5 are part of the "peripheral" site. Indeed, a higher EDR concentration ($>20 \mu\text{M}$) fully protects all seven massifs, presumably by occupying both active and peripheral sites (not shown). The first five massifs, accounting for 71% of specifically incorporated radioactivity, were resolved into several peaks (not shown). Edman degradation revealed a major amino acid sequence in each peak.

In all peaks of massifs 4 and 5, the residue labeled was Trp-279. These peptides differed in length, but all contained the sequence PQELIDVEWN, and heterogeneity was attributed to partial proteolysis. The radioactivity in these peaks represents 22% of the total radioactivity specifically incorporated. The greater part, 49%, was found on Phe-330 in peptides purified from massifs 1–3. These were also of

different lengths, but all contained the sequence, DEGSFF-LYG, corresponding to residues 326–334.

The labeling of Phe-330 supports the crystallographic data, as well as the previous assignment, based on labeling *Electrophorus* AcChoEase (24). Labeling of Trp-279, at the top of the gorge, is of especial interest in light of the crystallographic data showing that the distal quaternary group of DECA is close to the indole of this residue. Labeling of these two residues gains additional significance if one recalls that incorporation of one molecule of [^3H]DDF per active site suffices to block enzymic activity completely. This indicates that labeling of Trp-279 or Phe-330 is mutually exclusive and thus that the two sites are somehow coupled (see also ref. 28). While the direct role of Phe-330 in the active site seems clear, that of Trp-279 remains to be established. However, both its position at the top of the gorge and the data presented suggest that it may be regulating entry into the gorge. Replacement of Trp-279 by Ala, by site-directed mutagenesis, greatly reduces inhibition by the peripheral-site ligand propidium (28, 29). The "peripheral" anionic site may also be the substrate-binding site involved in substrate inhibition (27). The mutually exclusive labeling observed may thus be formally analogous to substrate inhibition.

Polar Interactions of Aromatic Residues. The differences in orientation of the aromatic ring of Phe-330 observed in the different ligand·AcChoEase complexes must clearly be taken into account in designing anticholinesterase drugs. Increasing evidence implicates π electrons of aromatic residues in polar interactions within proteins (30–32). Moreover, theoretical considerations and model host-guest studies invoke aromatic groups as a general feature of quaternary-ligand-binding sites (33, 34).

It is thus of interest to speculate whether conformational changes of the type induced in AcChoEase upon binding of various ligands may also occur upon ligand binding by nicotinic or muscarinic AcCho receptors or by receptors activated by biogenic amines bearing aromatic groups—e.g., epinephrine and serotonin. Photoaffinity labeling shows several aromatic rings to be involved in the AcCho-binding site of the nicotinic AcCho receptor (26). Labeling of some

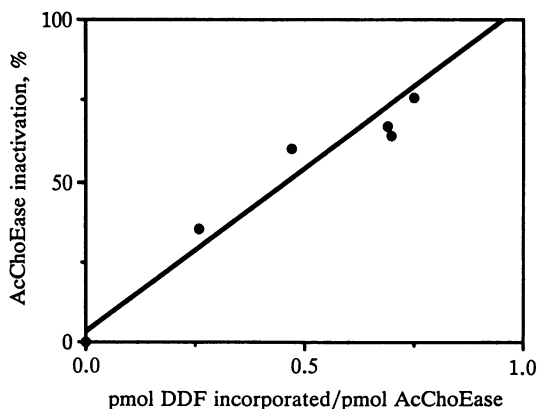


FIG. 3. Extent of AcChoEase inactivation as a function of [^3H]DDF incorporation. AcChoEase was irradiated in the presence of 40 μM [^3H]DDF for various times (3–20 min). For each point, radioactivity specifically incorporated was determined from HPLC profiles of tryptic digests.

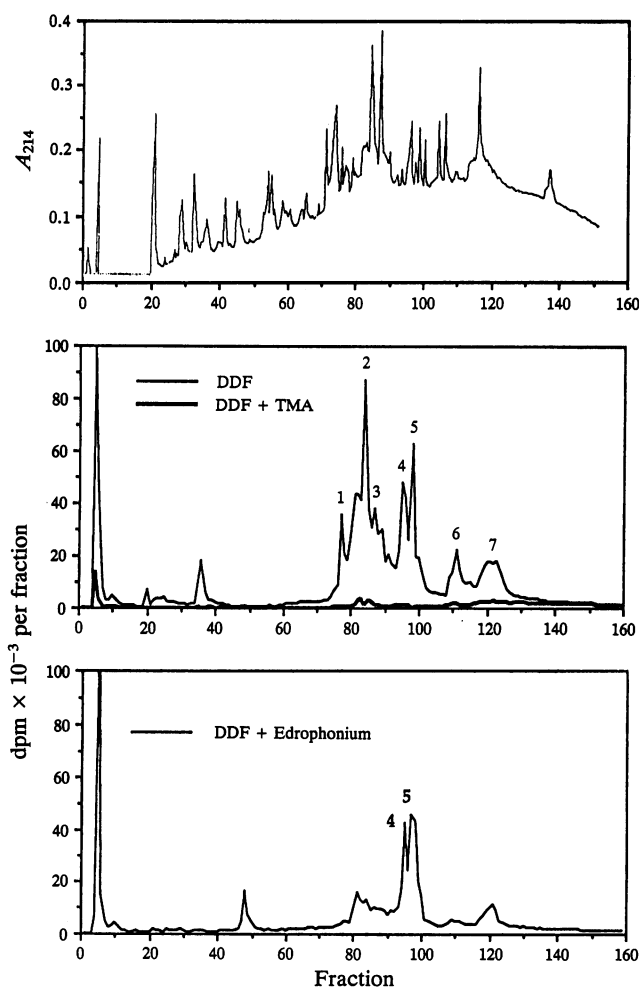


FIG. 4. Reversed-HPLC profile of $[^3\text{H}]$ DDF-labeled peptides. AcChoEase was irradiated in the presence of $40 \mu\text{M}$ $[^3\text{H}]$ DDF (with or without 0.1 M TMA or $5 \mu\text{M}$ EDR as protective agent). After irradiation, labeled AcChoEase was digested by 5% trypsin. Peptides were separated by HPLC and 0.75-ml (0.5-min) fractions were collected. Absorbance at 214 nm (Top) and radioactivity (Middle and Bottom) were monitored.

residues was increased in the desensitized state, suggesting that they may play a key role in the putative conformational changes involved in regulating ligand-gated ion channels (35). Both the specificity and conformational changes observed in the present study may thus have general significance for receptor function.

We thank Miriam Laschever, Felix Frolow, Mia Raves, Alexander Faibusovitch, and Lilly Toker for help in this research. This project was supported by U.S. Army Medical Research and Development Command Contract DAMD17-89-C-9063, the Centre National de la Recherche Scientifique, the Fondation pour la Recherche Médical, the Fondation de France, Association Franco-Israélienne pour la Recherche Scientifique et Technologique, the Minerva Foundation, and the Kimmelman Center. I.S. is Bernstein-Mason Professor of Neurochemistry. P.H.A. is supported by the L. P. Markey Charitable Trust.

1. Hobbiger, F. (1976) in *Handbuch der Experimentellen Phar-*

makologie, ed. Zaimis, E. (Springer, Berlin), Vol. 42, pp. 487–581.

2. Taylor, P. (1990) in *The Pharmacological Basis of Therapeutics*, eds. Gilman, A. G., Nies, A. S., Rall, T. W. & Taylor, P. (Macmillan, New York), 5th Ed., pp. 131–150.

3. Becker, R. E. & Giacobini, E. (1991) *Cholinergic Basis for Alzheimer Therapy* (Birkhaeuser, Boston).

4. Quinn, D. M. (1987) *Chem. Rev.* **87**, 955–975.

5. Changeux, J. P. (1966) *Mol. Pharmacol.* **2**, 369–392.

6. Taylor, P. & Lappi, S. (1975) *Biochemistry* **14**, 1989–1997.

7. Main, A. R. (1976) in *Biology of Cholinergic Function*, eds. Goldberg, A. M. & Hanin, I. (Raven, New York), pp. 269–353.

8. Bergmann, F. & Segal, R. (1954) *Biochem. J.* **58**, 692–698.

9. Mooser, G. & Sigman, D. S. (1974) *Biochemistry* **13**, 2299–2307.

10. Sussman, J. L., Harel, M., Frolow, F., Oefner, C., Goldman, A., Toker, L. & Silman, I. (1991) *Science* **253**, 872–879.

11. Shinitzky, M., Dudai, Y. & Silman, I. (1973) *FEBS Lett.* **30**, 125–128.

12. Goeldner, M. P. & Hirth, C. G. (1980) *Proc. Natl. Acad. Sci. USA* **77**, 6439–6442.

13. Weise, C., Kreienkamp, H.-J., Raba, R., Pedak, A., Aaviksaar, A. & Hucho, F. (1990) *EMBO J.* **9**, 3885–3888.

14. Bernstein, F. C., Koetzel, T. F., Williams, G. J. B., Meyer, E. F., Jr., Brice, M. D., Rodgers, J. R., Kennard, O., Schimnouchi, T. & Tasumi, M. (1977) *J. Mol. Biol.* **112**, 535–542.

15. Ehret-Sabatier, L., Schalk, I., Goeldner, M. & Hirth, C. (1992) *Eur. J. Biochem.* **203**, 475–481.

16. Sussman, J. L., Harel, M., Frolow, F., Varon, L., Toker, L., Futerman, A. H. & Silman, I. (1988) *J. Mol. Biol.* **203**, 821–823.

17. Brünger, A. T. (1990) *x-PLOR, A System for Crystallography and NMR* (Yale Univ., New Haven, CT), 3.0 Manual.

18. Ellman, G. L., Courtney, K. D., Andres, V., Jr., & Featherstone, R. M. (1961) *Biochem. Pharmacol.* **7**, 88–95.

19. Wilson, I. B. & Quan, C. (1958) *Arch. Biochem. Biophys.* **73**, 131–143.

20. Heilbronn, E. (1961) *Acta Chem. Scand.* **15**, 1386–1390.

21. Gauthier, S. & Gauthier, L. (1991) in *Cholinergic Basis of Alzheimer Therapy*, eds. Becker, R. & Giacobini, E. (Birkhaeuser, Berlin), pp. 224–230.

22. Zaimis, E. & Head, S. (1976) in *Handbuch der Experimentellen Pharmakologie*, ed. Zaimis, E. (Springer, Berlin), Vol. 42, pp. 365–419.

23. Langenbuch-Cachat, J., Bon, C., Mülle, C., Goeldner, M., Hirth, C. & Changeux, J.-P. (1988) *Biochemistry* **27**, 2337–2345.

24. Kieffer, B., Goeldner, M., Hirth, C., Aebersold, R. & Chang, J. Y. (1986) *FEBS Lett.* **202**, 91–96.

25. Dennis, M., Giraudat, J., Kotzyba-Hibert, F., Goeldner, M., Hirth, C., Chang, J.-Y., Lazure, C., Chrétien, M. & Changeux, J.-P. (1988) *Biochemistry* **27**, 2346–2357.

26. Galzi, J.-L., Revah, F., Black, D., Goeldner, M., Hirth, C. & Changeux, J.-P. (1990) *J. Biol. Chem.* **265**, 10430–10437.

27. Radic, Z., Reiner, E. & Taylor, P. (1991) *Mol. Pharmacol.* **39**, 98–104.

28. Shafferman, A., Velan, B., Ordentlich, A., Kronman, C., Grosfeld, H., Leitner, M., Flashner, Y., Cohen, S., Barak, D. & Ariel, N. (1992) *EMBO J.* **11**, 3561–3568.

29. Harel, M., Sussman, J. L., Krejci, E., Bon, S., Chanal, P., Massoulié, J. & Silman, I. (1992) *Proc. Natl. Acad. Sci. USA* **89**, 10827–10831.

30. Burley, S. K. & Petsko, G. A. (1985) *Science* **229**, 23–28.

31. Axelsen, P. H., Gratton, E. & Prendergast, F. G. (1991) *Biochemistry* **30**, 1173–1179.

32. Sussman, J. L. & Silman, I. (1992) *Curr. Opin. Struct. Biol.* **2**, 721–729.

33. Dougherty, D. A. & Stauffer, D. A. (1990) *Science* **250**, 1558–1560.

34. Verdonk, M. L., Boks, G. J., Kooijman, H., Kanters, J. A. & Kroon, J. (1993) *J. Computer-Aided Mol. Design* **7**, 173–182.

35. Galzi, J.-L., Revah, F., Bouet, F., Ménez, A., Goeldner, M., Hirth, C. & Changeux, J.-P. (1991) *Proc. Natl. Acad. Sci. USA* **88**, 5051–5055.